

IoT-BASED EVAPOTRANSPIRATION ESTIMATION OF PEANUT PLANT USING DEEP NEURAL NETWORK

/

ESTIMASI EVAPOTRANSPIRASI TANAMAN KACANG TANAH BERBASIS IoT MENGGUNAKAN DEEP NEURAL NETWORK

Suhardi^{1,2)}, Bambang Marhaenanto¹⁾, Bayu Taruna Widjaja Putra^{1,*)}, Sugeng Winarso²⁾

¹⁾ Agricultural Engineering, Faculty of Agricultural Technology, University of Jember, Jember, Indonesia 68121

²⁾ Doctoral study program in agricultural science, Faculty of Agriculture, University of Jember, Jember, Indonesia 68121

*Corresponding Author E-mail: bayu@unej.ac.id

DOI: <https://doi.org/10.35633/inmateh-70-47>

Keywords: DNN, evapotranspiration, NDVI, sensors, temperature, humidity

ABSTRACT

The water availability in soil strongly influences crop growth by sustaining photosynthesis, respiration, and the maintenance of plant temperature. The water availability will decrease due to crop evapotranspiration (ET_c) which is influenced by reference evapotranspiration (ET_o) and crop coefficient (K_c). During water shortage, K_c is strongly influenced by soil evaporation coefficient (K_e) and basal crop coefficient (K_{cb}) which can be calculated using the Blue Red Vegetation Index (BRVI). The purpose of this study was to apply and evaluate a new method of estimating ET_o, K_e, and K_{cb} at a research site using a Deep Neural Network (DNN) with minimum requirements. The results of the ET_o estimation using DNN shows a good output with a determinant coefficient (R²) being 0.774. Meanwhile, the estimates of K_e and K_{cb} show excellent results with the determinant coefficient (R²) being 0.9496 and 0.999 respectively.

ABSTRAK

Ketersediaan air dalam tanah sangat mempengaruhi pertumbuhan tanaman untuk mempertahankan fotosintesis, respirasi, dan pemeliharaan suhu tanaman. Ketersediaan air akan berkurang akibat evapotranspirasi tanaman (ET_c) yang dipengaruhi oleh evapotranspirasi referensi (ET_o) dan koefisien tanaman (K_c). Pada saat kekurangan air, K_c sangat dipengaruhi oleh koefisien penguapan tanah (K_e) dan basal crop koefisien (K_{cb}) yang dapat dihitung dengan menggunakan Normalized Difference Vegetation Index (NDVI). Tujuan dari penelitian ini adalah untuk menerapkan dan mengevaluasi metode baru estimasi ET_o, K_e, dan K_{cb} di lokasi penelitian menggunakan Deep Neural Network (DNN) dengan persyaratan minimum. Hasil estimasi ET_o menggunakan DNN menunjukkan output sangat baik dengan koefisien determinan (R²) 0.774. Sementara itu, estimasi K_e dan K_{cb} menghasilkan luaran sangat baik dengan koefisien determinan (R²) secara berurutan adalah 0.9496 dan 0.999.

INTRODUCTION

One of the factors that affect crop growth is the availability of water which functions as a solvent and medium for biochemical reactions, a raw material for photosynthesis, and a determinant to maintain constant crop temperature. Water availability is extremely dependent on rainwater because some of the rainwater that seeps into the ground will be stored in it. However, water in the soil will be increasingly limited during the dry season due to increased temperature which subsequently raises evapotranspiration. Likewise, solar radiation and wind speed are likely to increase evapotranspiration (Luo et al., 2021) (Dong et al., 2020) (Kiefer et al., 2019). On the other hand, relative humidity (RH) is the ratio between actual water vapor pressure and saturated water vapor pressure at a specific temperature which affects the decrease in evapotranspiration when RH increases (Fu et al., 2022). Other factors that affect evapotranspiration are environmental factors, such as the nature of vegetation and anthropogenic management (Jiao et al., 2019). Given these driving factors to water availability, researchers generally analyze temperature, solar radiation, humidity, wind speed, and rainfall to estimate evapotranspiration using Artificial Neural Networks (ANN) (Vulova et al., 2021; Ferreira & França, 2020; Elbeltagi et al., 2020; Ferreira et al., 2019; Saggi and Jain, 2019).

The estimation of evapotranspiration using an ANN with a big dataset produces very good results. However, ANN-based evapotranspiration estimation with small dataset can also be a promising option in the absence of big datasets (Feng et al., 2019).

In this direction, this study investigated the use of the minimum dataset requirement involving T_{mean} and RH_{mean} to estimate evapotranspiration. In addition, T_{mean} and RH_{mean} datasets, BRVI, and basal crop coefficient (K_{cb}) from the FAO table in one growing season were used as input parameters to estimate the K_{cb} of sample crops and soil evaporation coefficient (K_e) on the research site.

In this scenario, this study aimed to apply and evaluate a new model of evapotranspiration estimation using DNN with a minimum dataset requirement based on the Internet of Things (IoT).

MATERIALS AND METHODS

Research site

The research site was located at the University of Jember, East Java, Indonesia, located at -8.16346° and 113.71305° with a tropical climate and two seasons, the rainy season and dry season. The beginning of the rainy season occurs in September, while the dry season begins in April. In this dry season, the water availability in the soil decreases, so some crops do not receive sufficient water supply through irrigation. This has an impact on crop growth and yields.

Datasets

This study used data on temperature (T), relative humidity (RH), K_{cb} from the FAO table, and BRVI from crop images recorded by cameras based on the Internet of Things (IoT) from January 2022 to April 2022. Peanut plants were used as samples in this study. T_{mean} and RH_{mean} generated through a 4-hour data recording served as input data for DNN-based E_{To} estimation. Meanwhile, E_{To} from the IoT-based lysimeter measurement was compared against the estimated output of E_{To} . The T_{mean} , RH_{mean} , and K_{cb} from the FAO table and BRVI in one growing season were used as input data to estimate the soil evaporation coefficient (K_e) and K_{cb} of crops on the research site. Temperature and humidity sensors were used to record T and RH. Meanwhile, the load cell sensor was used as an IoT-based grass crop weight sensor to measure E_{To} . The change in the weight of grass and soil was considered as the weight of evapotranspiration of water and converted to the actual E_{To} height. Temperature and humidity sensors were placed around the crop while the growing media and crops were placed on top of the load cell. The node MCU ESP8266 module which functioned as an internet connection microcontroller was used for recording T , RH, and E_{To} and sending these data to a cloud server.

Peanut images were captured using a camera sensor placed above the crop canopy by attaching it to a pole. The camera was put next to the crop to capture RGB data directly on the crop leaves (Putra et al., 2020). Red (R) and blue (B) bands in the image crops were used for BRVI calculations (Delalieux et al., 2023). The specifications of camera sensor, T and RH sensor, and load cell sensor are presented in Table 1, and the equipment arrangement is shown in Figure 1.

Table 1

Specification of the camera sensor, temperature sensor, humidity sensor, and load cell sensor

Sensor	Specification
Camera sensor module	<ul style="list-style-type: none"> Connectivity using WiFi 802.11b/g/n, Bluetooth 4.2 with BLE. Microcontroller computing power up to 600 DMIPS. The memory storage of 520KB SRAM + 4MB PSRAM + SD card slot. A 9-pin GPIO port. 2MP camera with JPEG image format. An external FTDI adapter to connect the camera, sensor module to the mini-USB port.
Temperature (T) and relative humidity (RH) sensors	<ul style="list-style-type: none"> Measuring range of 20-90% RH and temperature 0-50°C. Measurement accuracy of $\pm 5\%$ RH and $\pm 2^\circ\text{C}$. Voltage source of 5V DC. Current consumption of 0.5mA-2.5mA.
Load cell	<ul style="list-style-type: none"> Aluminum alloy as basic material Dimensions 8x1.25x1.25 cm Operating temperature range of -20°C – 65°C Output of 0.1mV - 1mV/V The margin of error $\leq 1.5\%$

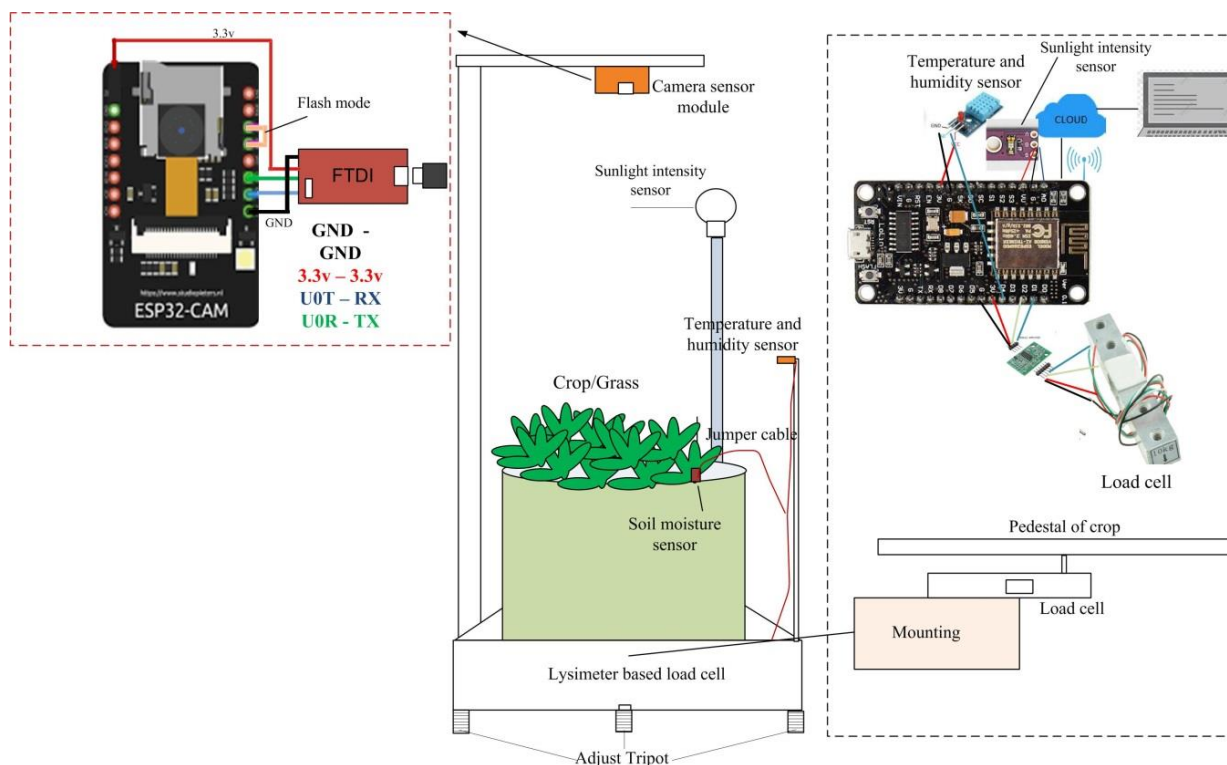


Fig. 1 - The arrangement of camera sensor equipment, weighting lysimeter device, IoT-based temperature, and humidity sensor

The estimation of Kcb using BRVI

The estimation of Kcb of peanut plants on the research site was done by identifying a linear relationship between the NDVI and the FAO Kcb of peanut plants, while the NDVI of peanut plants was calculated by equation 1. Furthermore, the NDVI was plotted with the Kcb from the FAO table (Kcb-FAO) at the same plant phase and age (Reyes-gonzález *et al.*, 2018; Sánchez *et al.*, 2021; de Oliveira *et al.*, 2020). The relationship between NDVI and Kcb was based on the fact that NDVI will tend to increase until the development stage and decrease at the late season stage (harvest). Likewise, Kcb tends to rise in the initial stage up to the development stage, but it is likely to decrease in the late season stage. As an alternative, a scatter plot in the form of a triangle between Land Surface Air Temperature (LST) and NDVI can be used to estimate Kcb (Chen and Liu, 2020). The resultant linear equation was used as the basis for calculating the Kcb-NDVI value (Niu *et al.*, 2020). On the other hand, the use of RGB cameras for taking plant images has been widely used to diagnose plant physiological characteristics including leaf chlorophyll content (Liu *et al.*, 2021). B and R bands on the RGB camera image are used to calculate the Blue Red Vegetation Index (BRVI) which functions to assess the biophysical properties of the vegetation index. Therefore, BRVI is identical to the NDVI value calculated using the NIR and R band (Putra and Soni, 2017).

$$BRVI = \frac{(B-R)}{(B+R)} \quad (1)$$

The accuracy rate of Kcb estimation can be justified by referring to the correlation coefficient. A very good correlation is marked by coefficient index ranging from 0.9 to 1.0, a range of 0.70 to 0.89 is a good correlation, a range of 0.40 to 0.69 denotes a moderate correlation, and a range of 0.1 – 0.39 indicates weak correlation (Schober *et al.*, 2018).

The estimation of ETo using DNN

The estimation of evapotranspiration using DNN employed an architecture involving 1 input layer, 4 hidden layers, and 1 output layer with a Rectified Linear Unit (ReLU) activation function. The ReLU activation function was chosen because it has a better performance than sigmoid logistics (Huang *et al.*, 2019). Meanwhile, the data compositions for DNN modeling at the training and testing stages were 70% and 30% respectively.

The DNN-based estimation of ETo using minimum dataset requirement

This research engaged minimum dataset requirements comprising Tmean, RHmean, and the actual ETo measurement results of an IoT-based lysimeter within 7 days of data recording, with a duration of 4 hours each day. The input data were Tmean and Rhmean while ETo was used as comparison data against DNN output.

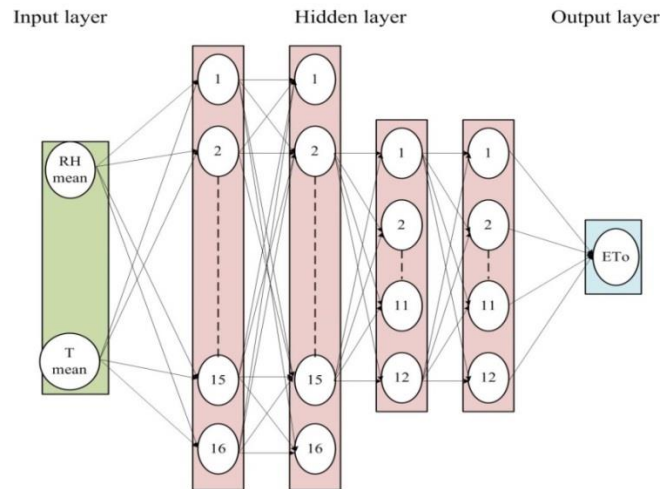


Fig. 2 - DNN architecture for ETo estimation using minimum dataset requirement.

The estimation of Kcb and Ke

Changes in crop growth from the initial planting to harvesting were indicated by Kcb. The Kcb at the initial stage was constant and started to rise during the development stage. The Kcb remained constant until the mid-season stage, but it sank until the late season stage. Meanwhile, the Ke can be derived from NDVI and a fraction of vegetation cover (Fc), such as equations 3 and 4 (Zhang et al., 2019; Wang T. et al., 2021). In general, the Fc value of FAO (Fc-FAO) in each crop stage was described as follows: (a) initial stage (0 – 0.1); (b) crop development stage (0.1 – 0.8); (c) mid-season stage (0.8 – 1); and (d) late season stage (0.8 - 0.2) (Allen et al., 1998).

$$Ke = 0.9 * (1 - Fc) \tag{2}$$

$$Fc = 1.19 * (NDVI - NDVimin) \tag{3}$$

$$Fc = 1.26 * NDVI - 0.18 \tag{4}$$

Based on this description, Tmean, RHmean, and BRVI of the peanut plants were used as input data to estimate Kcb and Ke with the aid of DNN. The target data which included Kcb-BRVI and Ke-FAO served as comparative data against the DNN output. Kcb-BRVI was generated from the linear equation between Kcb, FAO tables, and BRVI, while Ke was generated from equation 2. The DNN architecture is shown in Figure 3.

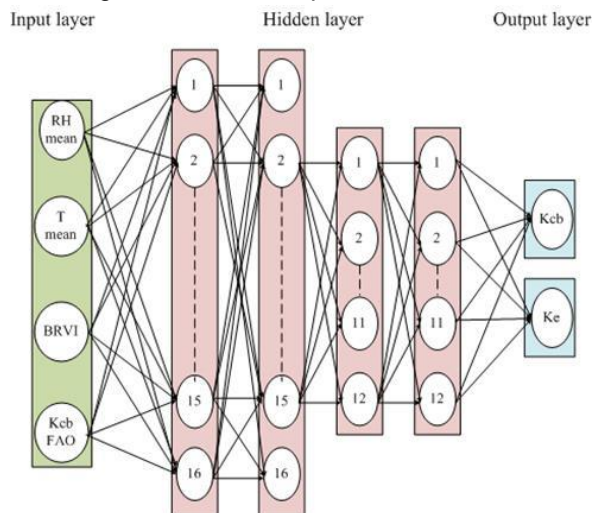


Fig. 3 - DNN Architecture of Kcb and Ke Estimation

RESULTS

RGB camera sensor calibration

RGB camera sensor was calibrated by calculating the relationship between the BRVI of the RGB camera sensor (BRVI-camera sensor) and the NDVI spectrometer (NDVI-spectrometer). The NDVI was generated by calculating the reflectance rate of the red and blue bands in the leaf samples. Meanwhile, the combination of RGB bands from the camera sensor had to be extracted first to produce red and blue bands, and then the red and blue band reflectance rate was calculated to estimate the BRVI. The calibration results demonstrate a very satisfactory accuracy with R^2 of 0.8973 (see Figure 4).

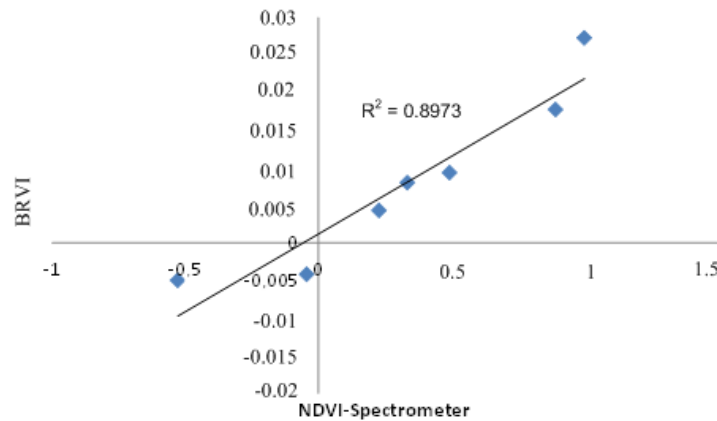


Fig. 4 - The result of camera sensor calibration

The estimation of Kcb using BRVI

The images of peanut plants were captured at different stages of plant growth, including the initial stage, development stage, and mid-season stage. Furthermore, the BRVI in the images was calculated using the QGIS 3.10 software as shown in Figure 5.

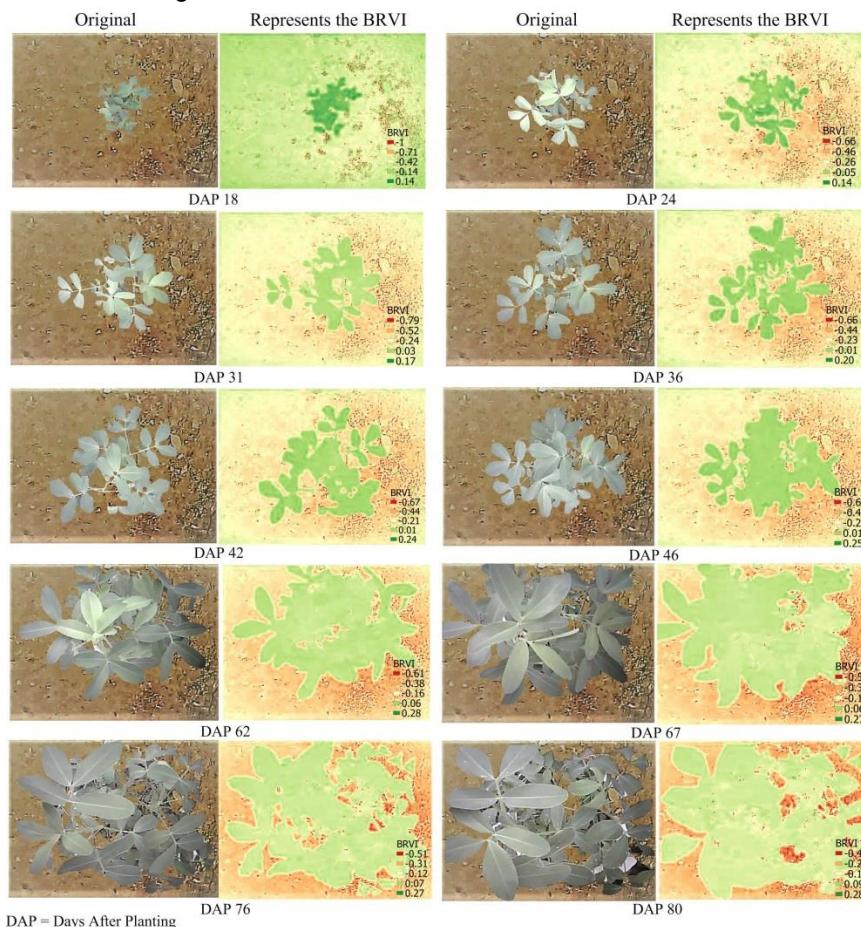


Fig. 5 - The calculation of the NDVI-RGB of peanut plant images from the initial stage to mid-season stage

The calculation results of the BRVI from the peanut plant images using a camera sensor indicated similar trend between the BRVI and Kcb-FAO. The trend was marked by constant value in the initial stage and an increase in the development stage, but constant value was restored in the mid-season stage. This shows a very strong correlation between BRVI and Kcb-FAO, as indicated by R^2 of 0.8748 (Figure 6). By implication, BRVI can be used to estimate the Kcb of peanut plants. This finding resonates with previous research reporting that the NDVI and Kcb of plants were positively correlated (Niu *et al.*, 2020). In harmony, another study confirms that NDVI can be used to estimate Kc on the field in all plant phases (Zhang *et al.*, 2019).

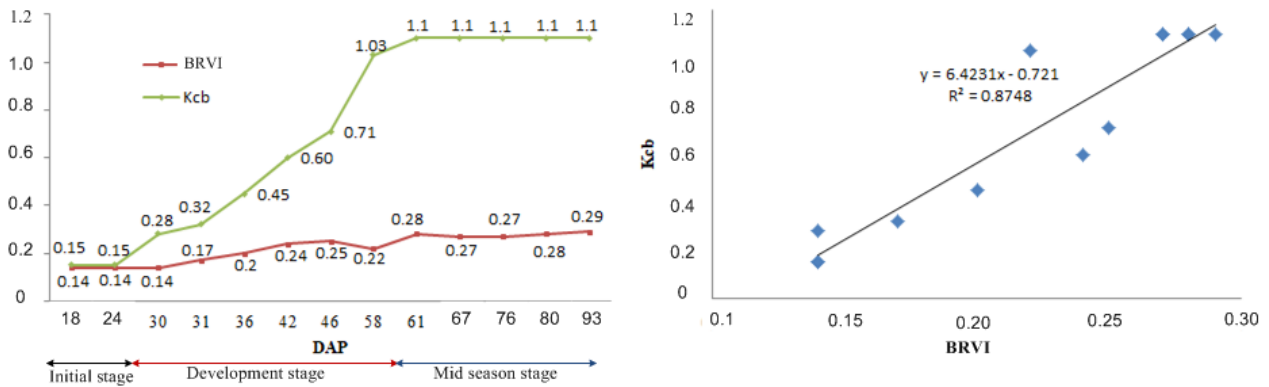


Fig. 6 - The trends of BRVI and Kcb-FAO in peanut

The estimation of ETo using minimum dataset requirements

ETo estimation based on DNN used a minimum requirement dataset in the form of Tmean, RHmean, and actual ETo recorded every 4 hours from January 8th, 2022 to January 15th, 2022. Input and target data are presented in Figure 7, while the ETo estimation results can be seen in Figures 8 and 9.

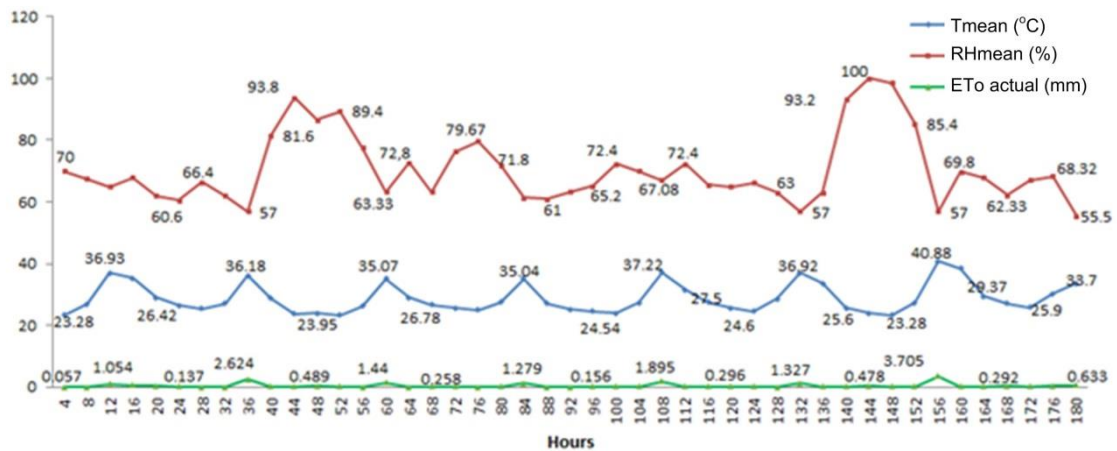


Fig. 7 - Input and target data for estimating ETo using DNN

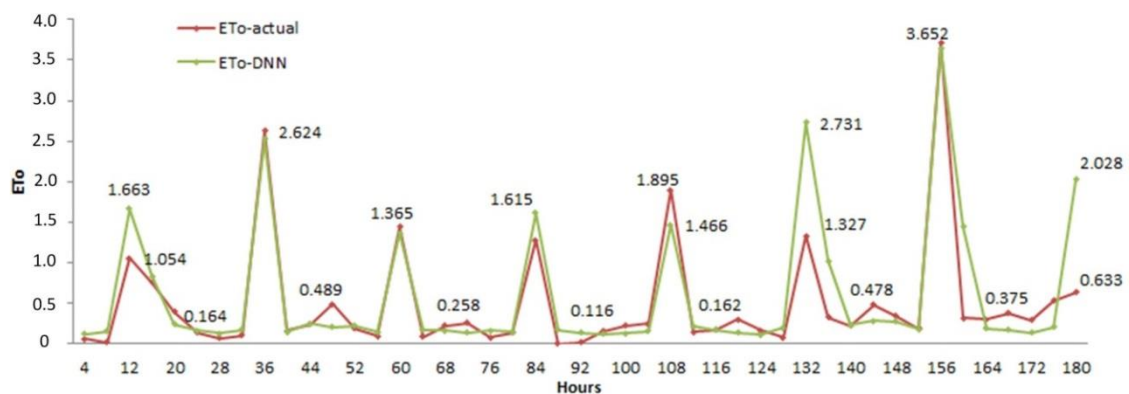


Fig. 8 - ETo estimation using DNN with minimum dataset requirements

Based on Figure 7, the trend of ETo is similar to that of Tmean but different from that of Rhmean. Tmean and ETo tend to increase simultaneously. On the other hand, when RHmean increases, ETo tends to decrease. This is coherent with a previous research which states that an increase in temperature increases ETo, but an increase in RH has the opposite effect (Luo et al., 2021). Figure 8 shows that ETo estimation using DNN with Tmean and RHmean as input data using 4 hidden layers (16-16-12-12) shows very good results. This is indicated by the trend associated with ETo-DNN, which is equal to the actual ETo. The ETo-DNN and actual ETo were relatively the same and coincided at 36, 60, and 156 hours respectively. The DNN using 4 hidden layers (16-16-12-12) with the ReLU activation function demonstrates a very good performance at epoch 1000 with a (mean absolute error) MAE of 0.1412 and R² of 0.7704 as shown in Figure 9.

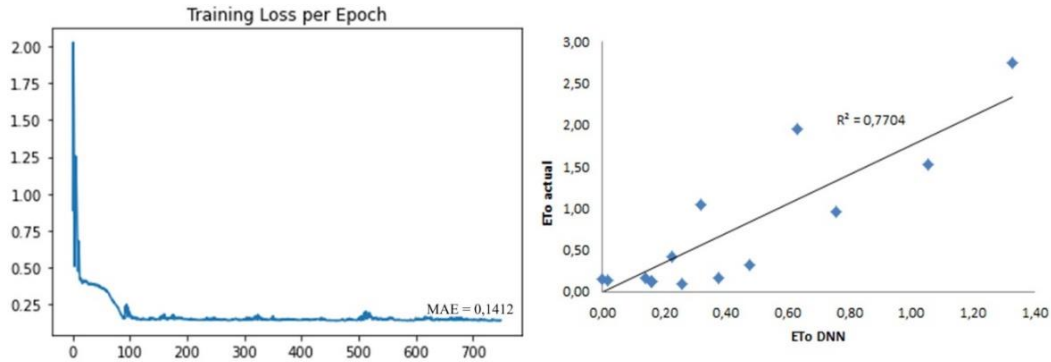


Fig. 9 - MAE and R² of ETo Estimation Using DNN with Minimum Dataset Requirement

The estimation of Kcb and Ke using DNN

From the initial stage to the late season stage, Tmean, RHmean, Kcb-FAO, and BRVI of peanut plants were recorded as input data to estimate Kcb and Ke. Kcb resulting from the BRVI transformation (Kcb-BRVI) and Ke-FAO calculated using equation 2 was used as a comparison against Kcb-DNN and Ke-DNN. The input and output data for the estimation of Kcb and Ke using DNN are presented in Figure 10 and Figure 11.

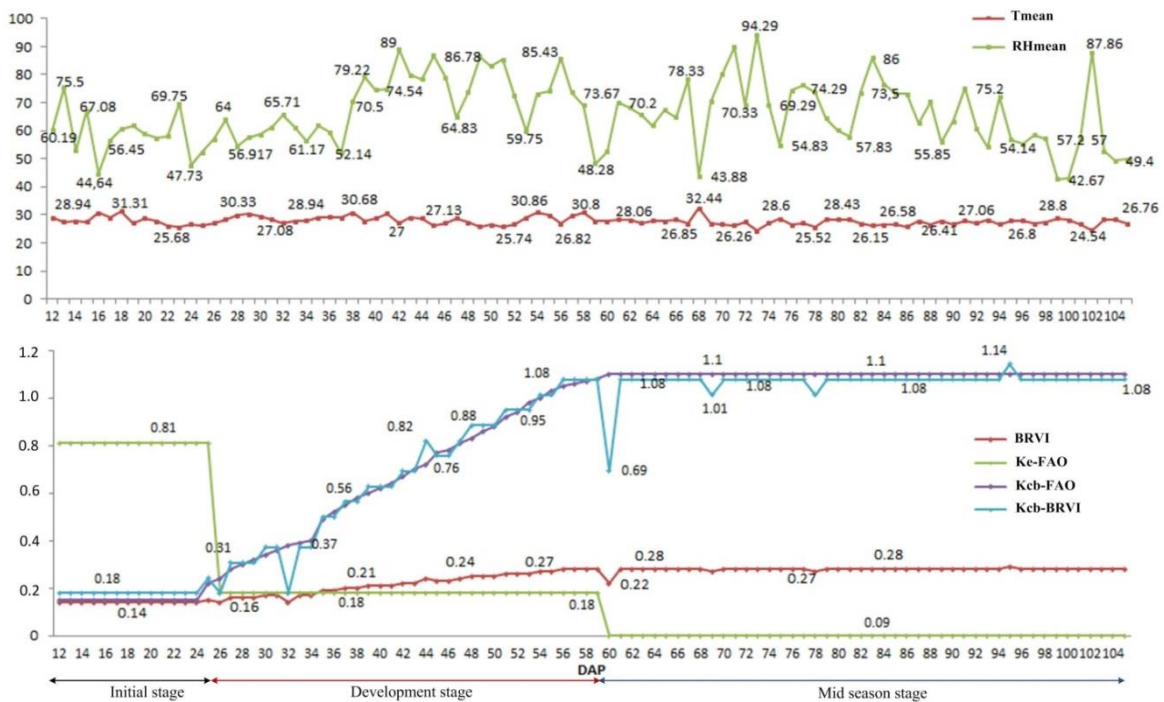


Fig. 10 - Dataset to estimate Kcb and Ke using DNN

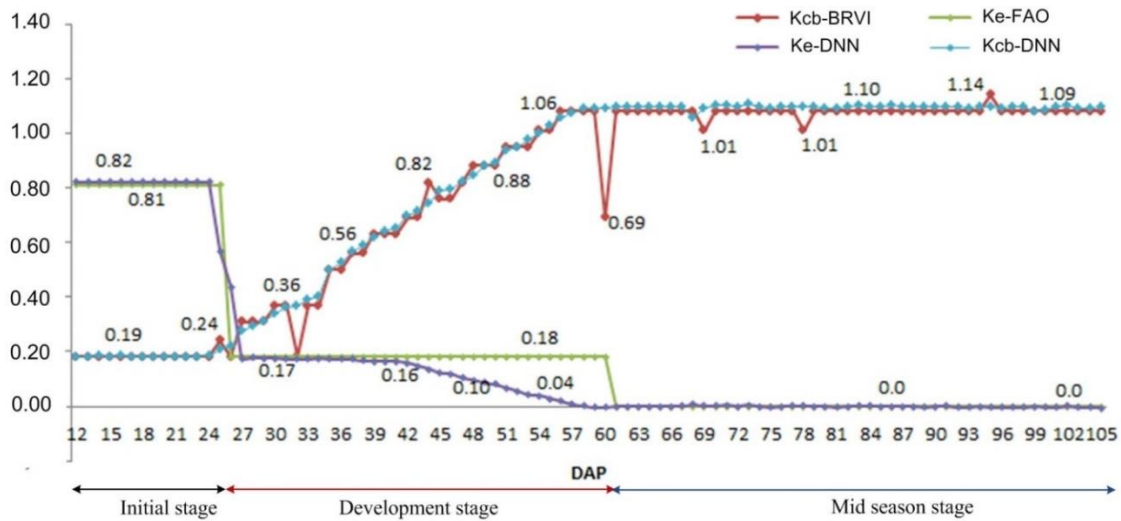


Fig. 11 - The trends of Kcb and Ke estimated using DNN

Figure 11 shows a very decent trend of Kcb and Ke as estimated using DNN with input data involving Tmean, RHmean, Kcb-FAO, and BRVI. Similar trends are identified between Kcb-DNN and Ke-DNN, and these trends coincide with those of Kcb-BRVI and Ke-FAO. Decent DNN performance was achieved at epoch 2500 with MAE of 0.021 as well as R^2 of 0.9496 and 0.999, respectively (Figure 12). Thus, the DNN model with 4 parameters in the input layer and 4 hidden layers (16-16-12-12) can be used to estimate Kcb and Ke.

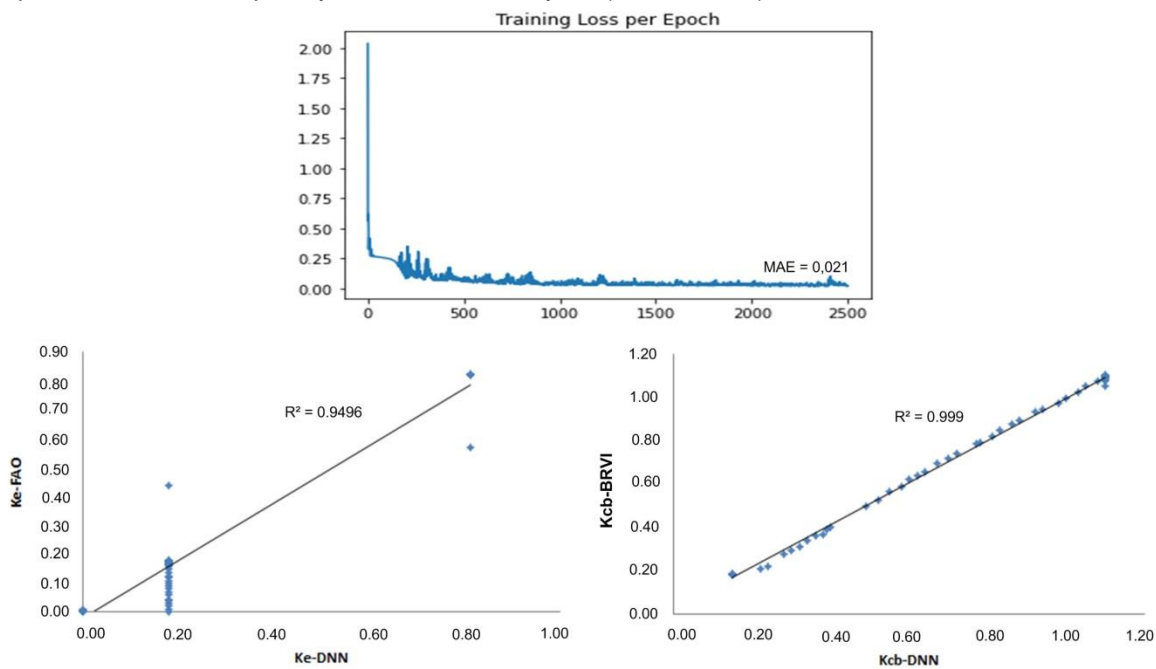


Fig. 12 - MAE and R^2 of Kcb and Ke estimation using DNN

CONCLUSIONS

The estimation of ETo using DNN with minimum dataset requirements can achieve highly accurate output. In this study, the minimum dataset requirements were Tmean and RHmean recorded from January 8th, 2022 to January 15th, 2022 (7 days) with 4 hours of data generation each day. This estimation has resulted in MAE of 0.1412 and R^2 of 0.7704. The findings demonstrate that ETo-DNN can be used as the basis for determining water requirements of crops in future studies. Likewise, the estimation of Ke and Kcb using DNN with datasets including Tmean, RHmean, Kcb-FAO, and BRVI report satisfactory accuracy rate, with MAE of 0.021 and R^2 of 0.9596 and 0.999 respectively. This confirms that Kcb-DNN and Ke-DNN can serve as a reference in calculating ETC in peanut plant.

ACKNOWLEDGEMENT

The author would like to thank mentors, especially families and all who have contributed to this research.

REFERENCES

- [1] Allen, R. G., S.Pereira, L., Raes, D., & Smith, M. (1998). FAO Irrigation and Drainage Paper No. 56. In *Food and Agriculture Organization of the United Nations* (Vol.13, Issue 3). FAO - Food and Agriculture Organization of the United Nations. [https://doi.org/10.1016/S0141-1187\(05\)80058-6](https://doi.org/10.1016/S0141-1187(05)80058-6)
- [2] Chen, J. M., & Liu, J. (2020). Evolution of evapotranspiration models using thermal and shortwave remote sensing data. *Remote Sensing of Environment*, 237 (December 2019), 111594. <https://doi.org/10.1016/j.rse.2019.111594>
- [3] Delalieux, S., Hardy, T., Ferry, M., Gomez, S., Kooistra, L., Culman, M., & Tits, L. (2023). Red Palm Weevil Detection in Date Palm Using Temporal UAV Imagery. *Remote Sensing*, 15(5), 1–21. Retrieved from <https://doi.org/10.3390/rs15051380>
- [4] de Oliveira, R. M., da Cunha, F. F., da Silva, G. H., Andrade, L. M., de Moraes, C. V., Ferreira, P. M. O., Raimundi, F. P. G., de Jesus Freitas, A. R., de Souza, C. M., & de Oliveira, R. A. (2020). Evapotranspiration and crop coefficients of Italian zucchini cultivated with recycled paper as mulch. *PLoS ONE*, 15(5), 1–16. <https://doi.org/10.1371/journal.pone.0232554>
- [5] Dong, W., Li, C., Hu, Q., Pan, F., Bhandari, J., & Sun, Z. (2020). Potential Evapotranspiration Reduction and Its Influence on Crop Yield in the North China Plain in 1961-2014. *Hindawi Advances in Meteorology*, 2020, 10. <https://doi.org/10.1155/2020/3691421>
- [6] Elbeltagi, A., Deng, J., Wang, K., Malik, A., & Maroufpoor, S. (2020). Modeling long-term dynamics of crop evapotranspiration using deep learning in a semi-arid environment. *Agricultural Water Management*, 241(March), 106334. <https://doi.org/10.1016/j.agwat.2020.106334>
- [7] Feng, S., Zhou, H., & Dong, H. (2019). Using deep neural network with small dataset to predict material defects. *Materials and Design*, 162, 300–310. <https://doi.org/10.1016/j.matdes.2018.11.060>
- [8] Ferreira, L. B., da Cunha, F. F., de Oliveira, R. A., & Fernandes Filho, E. I. (2019). Estimation of reference evapotranspiration in Brazil with limited meteorological data using ANN and SVM – A new approach. *Journal of Hydrology*. <https://doi.org/10.1016/j.jhydrol.2019.03.028>
- [9] Ferreira, L. B., & França, F. (2020). New approach to estimate daily reference evapotranspiration based on hourly temperature and relative humidity using machine learning and deep learning. *Agricultural Water Management*, 234(February), 106113. <https://doi.org/10.1016/j.agwat.2020.106113>
- [10] Fu, J., Gong, Y., Zheng, W., Zou, J., Zhang, M., Zhang, Z., Qin, J., Liu, J., & Quan, B. (2022). Spatial-temporal variations of terrestrial evapotranspiration across China from 2000 to 2019. *Science of the Total Environment*, 825, 153951. <https://doi.org/10.1016/j.scitotenv.2022.153951>
- [11] Huang, X., Gao, L., Crosbie, R. S., Zhang, N., Fu, G., & Doble, R. (2019). Groundwater recharge prediction using linear regression, multi-layer perception network, and deep learning. *Water (Switzerland)*, 11(9), 19. <https://doi.org/10.3390/w11091879>
- [12] Jiao, L., Lu, N., Fang, W., Li, Z., Wang, J., & Jin, Z. (2019). Determining the independent impact of soil water on forest transpiration: A case study of a black locust plantation in the Loess Plateau, China. *Journal of Hydrology*. <https://doi.org/10.1016/j.jhydrol.2019.03.045>
- [13] Kiefer, M. T., Andresen, J. A., Doubler, D., & Pollyea, A. (2019). Development of a gridded reference evapotranspiration dataset for the Great Lakes region. *Journal of Hydrology: Regional Studies*. <https://doi.org/10.1016/j.ejrh.2019.100606>
- [14] Liu, Y., Hatou, K., Aihara, T., Kurose, S., Akiyama, T., Kohno, Y., ... Omasa, K. (2021). A Robust Vegetation Index Based on Different UAV RGB Images to Estimate SPAD Values of Naked Barley Leaves. *Remote Sensing*, 13(4), 1–21.
- [15] Luo, Y., Gao, P., & Mu, X. (2021). Influence of meteorological factors on the potential evapotranspiration in Yanhe River Basin, China. *Water (Switzerland)*, 13(9), 1–13. <https://doi.org/10.3390/w13091222>
- [16] Niu, H., Wang, D., & Chen, Y. Q. (2020). Estimating Crop Coefficients Using Linear and Deep Stochastic Configuration Networks Models and UAV-Based Normalized Difference Vegetation Index (NDVI). *2020 International Conference on Unmanned Aircraft Systems, ICUAS 2020*, 1485–1490. <https://doi.org/10.1109/ICUAS48674.2020.9213888>

- [17] Putra, B. T. W., & Soni, P. (2017). Evaluating NIR-Red and NIR-Red edge External Filters with Digital Cameras for Assessing Vegetation Indices Under Different Illumination. *Infrared Physics and Technology*, 81, 148–156. <https://doi.org/10.1016/j.infrared.2017.01.007>
- [18] Putra, B. T. W., Soni, P., Marhaenanto, B., Pujiyanto, Sisbudi Harsono, S., & Fountas, S. (2020). Using Information from Images for Plantation Monitoring: A Review of Solutions for Smallholders. *Information Processing in Agriculture*, 7(1), 109–119. <https://doi.org/10.1016/j.inpa.2019.04.005>
- [19] Reyes-gonzález, A., Kjaersgaard, J., Trooien, T., Hay, C., Ahiablame, L., Nacional, I., & Agr, D. I. (2018). Estimation of Crop Evapotranspiration Using Satellite Remote Sensing-Based Vegetation Index. *Advances in Meteorology*, 2018(1).
- [20] Saggi, M. K., & Jain, S. (2019). Reference evapotranspiration estimation and modeling of the Punjab Northern India using deep learning. *Computers and Electronics in Agriculture*, 156 (October 2018), 387–398. <https://doi.org/10.1016/j.compag.2018.11.031>
- [21] Sánchez, J. M., Simón, L., González-piqueras, J., Montoya, F., & López-urrea, R. (2021). Monitoring Crop Evapotranspiration and Transpiration / Evaporation Partitioning in a Drip-Irrigated Young Almond Orchard Applying a Two-Source Surface Energy Balance Model. *Water MDPI*, 13(73), 1–25.
- [22] Schober, P., Boer, C., & Schwarte, L. A. (2018). Correlation Coefficients: Appropriate Use and Interpretation. *Anesthesia & Analgesia*, 126(5), 1763–1768. <https://doi.org/10.1213/ANE.0000000000002864>
- [23] Vulova, S., Meier, F., Duarte, A., Quanz, J., Nouri, H., & Kleinschmit, B. (2021). Modeling urban evapotranspiration using remote sensing, flux footprints, and artificial intelligence. *Science of the Total Environment*, 786. <https://doi.org/10.1016/j.scitotenv.2021.147293>
- [24] Wang, L., Duan, Y., Zhang, L., Rehman, T. U., Ma, D., & Jin, J. (2020). Precise estimation of NDVI with a simple NIR sensitive RGB camera and machine learning methods for corn plants. *Sensors (Switzerland)*, 20(11), 1–15. <https://doi.org/10.3390/s20113208>
- [25] Zhang, Y., Han, W., Niu, X., & Li, G. (2019). Maize crop coefficient estimated from UAV-measured multispectral vegetation indices. *Sensors (Switzerland)*, 19(23), 1–17. <https://doi.org/10.3390/s19235250>